INSTITUTE OF PHYSICS PUBLISHING JOURNAL OF PHYSICS A: MATHEMATICAL AND GENERAL

J. Phys. A: Math. Gen. **38** (2005) L513–L518 doi:10.1088/0305-4470/38/29/L01

LETTER TO THE EDITOR

Nodal-line densities of chaotic quantum billiard modes satisfying mixed boundary conditions

M V Berry[1] **and H Ishio**[2]

[1] H H Wills Physics Laboratory, Tyndall Avenue, Bristol BS8 1TL, UK
[2] 211, Institute for Advanced Research, Nagoya University, Nagoya 464-8601, Japan

Received 18 April 2005, in final form 12 May 2005
Published 6 July 2005
Online at stacks.iop.org/JPhysA/38/L513

Abstract

Statistics of nodal lines for eigenmodes u in the stadium are computed, and compared with previously derived formulae for monochromatic boundary-adapted Gaussian random waves in the plane. These modes and random waves satisfy the Helmholtz equation, and mixed boundary conditions in which a linear combination of u and its normal derivative must vanish. For the density of nodal lines and the excess density of nodal lines arising from the boundary, the Gaussian model accurately describes the statistics of the billiard eigenfunctions.

PACS numbers: 02.50.–r, 03.65.Sq, 05.45.Mt

1. Introduction

Our purpose here is to test a recent extension [1] (section 2) of the Gaussian random-wave model for eigenstates of classically chaotic quantum billiards [2–8]. Previously [9], the Gaussian model was generalized to incorporate Dirichlet and Neumann boundary conditions. The extension [1] was a further generalization to include mixed boundary conditions. It revealed some surprising boundary-related phenomena, whose appearance in quantum billiard states, reported here, gives strong support to the random-wave model.

In quantum billiards (section 3), eigenstates $u_n(\mathbf{r})$ with wavenumber k_n in a domain D of the plane $\mathbf{r} = \{x, y\}$, with boundary ∂D, satisfy

$$\nabla^2 u_n + k_n^2 u_n = 0 \text{ in } D, \qquad k u_n \cos a + \mathbf{n} \cdot \nabla u_n \sin a = 0 \text{ in } \partial D. \tag{1}$$

Here $\mathbf{n}$ is the inward normal, and a (with $-\pi/2 < a \leqslant \pi/2$) parametrizes the boundary condition. Dirichlet conditions correspond to $a = 0$ and Neumann to $a = \pi/2$.

In the boundary-adapted Gaussian random model, using scaled coordinates $\mathbf{R} = \{X, Y\} = \{kx, ky\}$, the domain is approximated as the half-space $Y \geqslant 0$, so the boundary is the straight line $Y = 0$. Members of the ensemble of random waves, whose statistics are to be compared with those of the modes (1), are [1]

$$u(\mathbf{r}, a) = \frac{2}{\sqrt{J}} \sum_{j=1}^{J} \frac{[\sin(Y \sin\theta_j) - \tan a \sin\theta_j \cos(Y \sin\theta_j)]}{\sqrt{1 + \tan^2 a \sin^2\theta_j}} \cos(X \cos\theta_j + \phi_j). \tag{2}$$

This is a superposition of J ($\gg 1$) plane waves satisfying the Helmholtz equation and boundary condition (1) for $Y \geqslant 0$, travelling in directions θ_j equidistributed on $[0, \pi]$ with phases ϕ_j equidistributed on $[0, 2\pi]$.

2. Summary of theory [1]

The nodal density $\rho_{\mathrm{L}}(Y; a)$ to be calculated, normalized so that $\rho_{\mathrm{L}}(Y, a) \to 1$ for $Y \to \infty$, is defined by

$$\text{mean nodal line length per unit area} \equiv \frac{k}{2\sqrt{2}}\rho_{\mathrm{L}}(Y, a). \tag{3}$$

The average here is over the ensemble parameters θ_j and ϕ_j, or equivalently (since the ensemble is ergodic) over long thin strips between Y and $Y + \mathrm{d}Y$. Equation (3) incorporates the previously derived bulk density $k/(2\sqrt{2})$ for nodal lines of isotropic Gaussian random functions far from boundaries [10].

The theory (expressed in a slightly simpler form than in [1] and [9]) involves the following averages, derived using more general techniques developed earlier [10]:

$$\begin{aligned} B(Y, a) &\equiv \langle u^2 \rangle = 1 - \frac{2}{\pi}\int_0^{\pi/2} \mathrm{d}\theta\, \mathrm{Re}\, f(\theta, Y, a) \\ D_X(Y, a) &\equiv \left\langle \left(\frac{\partial u}{\partial X}\right)^2 \right\rangle = \frac{1}{2} - \frac{2}{\pi}\int_0^{\pi/2} \mathrm{d}\theta (\cos\theta)^2\, \mathrm{Re}\, f(\theta, Y, a) \\ K(Y, a) &\equiv \left\langle u\frac{\partial u}{\partial Y} \right\rangle = \frac{2}{\pi}\int_0^{\pi/2} \sin\theta\, \mathrm{Im}\, f(\theta, Y, a), \end{aligned} \tag{4}$$

where

$$f(\theta, Y, a) = \exp(2\mathrm{i}Y\sin\theta)\left(\frac{1 - \mathrm{i}\tan a \sin\theta}{1 + \mathrm{i}\tan a \sin\theta}\right). \tag{5}$$

The result is that the nodal line density is

$$\rho_{\mathrm{L}}(Y, a) = \frac{2}{\pi}\sqrt{\frac{2D_X}{B}}E\left(\frac{B(B-1) + K^2}{BD_X}\right), \tag{6}$$

where E denotes the complete elliptic integral (the definition is that of *Mathematica* [11]).

The long-range behaviour of the nodal density is

$$\rho_{\mathrm{L}}(Y, a) \approx 1 + \frac{\cos\left(2Y - 2a - \frac{1}{4}\pi\right)}{\sqrt{\pi Y}} - \frac{1}{32\pi Y} \qquad (Y \gg 1). \tag{7}$$

The Y^{-1} dependence of the leading non-oscillatory correction implies that when the excess $\rho_{\mathrm{L}} - 1$ is integrated to give the total excess nodal line length $L_{\mathrm{exc}}(Y, a)$ in a strip of height Y, the result diverges as $Y \to \infty$. Thus

$$L_{\mathrm{exc}}(Y, a) \equiv \int_0^Y \mathrm{d}\eta[\rho_{\mathrm{L}}(\eta, a) - 1] = \frac{\sin\left(2Y - 2a - \frac{1}{4}\pi\right)}{2\sqrt{\pi Y}} - \frac{\log Y}{32\pi} + C_{\mathrm{L}}(a) \quad (Y \gg 1), \tag{8}$$

where the numerically determined constant $C_{\mathrm{L}}(a)$ is shown in figure 12 of [1]. This divergence is surprising because it indicates a sense in which the effect of the boundary conditions persists far from ∂D; moreover, the leading-order (logarithmic) divergence is independent of the boundary-condition parameter a.

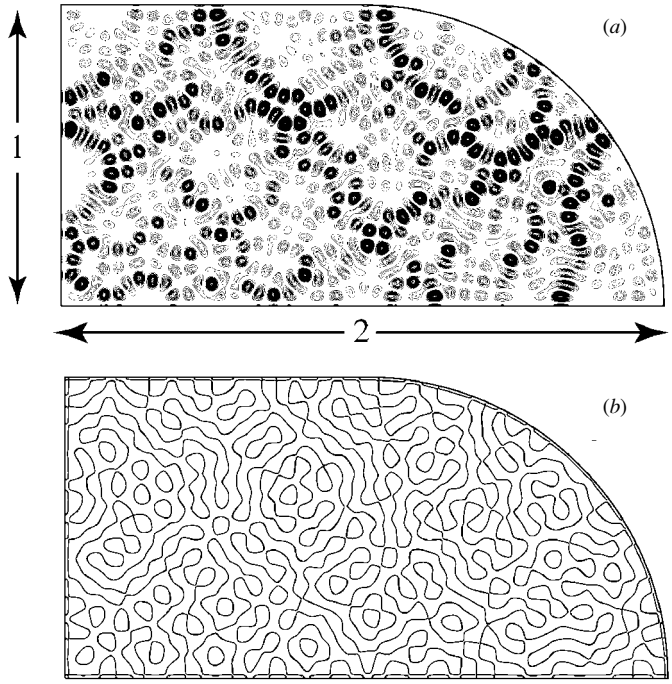

Figure 1. Pictures of the state $k = 83.89$ for $a = +\pi/4$. (*a*) Contour map of intensity $u^2(x, y)$ (the dark contour loops enclose regions of high intensity); (*b*) Nodal lines, showing 'ghost lines' [1] at a distance $ky \sim \pi/4$ from the boundary.

The other unanticipated feature of the theory is sharp peaks in $\rho_L(Y, a)$ near $Y = a$ for $(0 < a \ll \pi/2)$. In [1], these were discussed in detail and interpreted as ghosts of the boundary nodal line for $a = 0$.

In (7) and (8) the condition $Y \gg 1$ refers to the theoretical Gaussian-random superposition in the presence of a single straight boundary, and requires some qualification in the present application to quantum billiards. Y represents the shortest distance to ∂D, so Y/k should be much smaller than the local radius of curvature of ∂D, R, say. In fact we expect the theory of (7) and (8) to break down well before $Y = kR$, because the nodal density could feel the curvature and other non-local features of ∂D.

3. Stadium billiard

For D we chose the quarter stadium (figure 1) consisting of the unit square augmented by a quarter circle of radius 1. Thus the area A and perimeter P are

$$A = 1 + \tfrac{1}{4}\pi, \qquad P = 4 + \tfrac{1}{2}\pi. \tag{9}$$

For boundary-condition parameters $a = -\pi/4$, 0, $+\pi/4$, $+\pi/2$, we calculated eigenstates in the range $83 < k < 85$. According to the leading-order Weyl rule, this interval includes approximately 47 states, between the 978th and the 1026th. We used a mixed-boundary-condition adaptation of the numerical technique of Heller [6], in which k is varied so as to fit a superposition of N plane waves to the boundary conditions at N points on ∂D. It is easy to create combinations of the type (2) satisfying the mixed boundary conditions exactly on both straight sides of the quarter stadium; we chose $N = 320$ such combinations and fitted

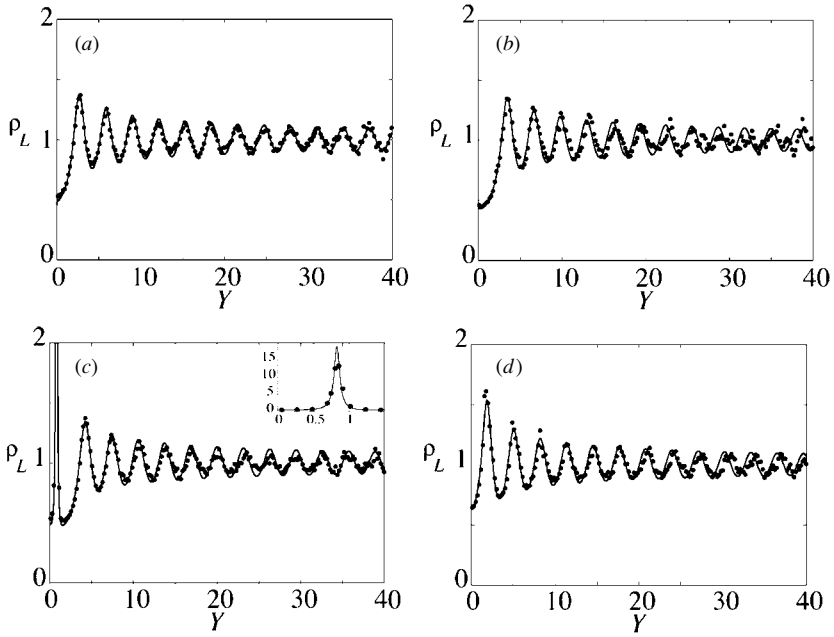

Figure 2. Nodal line density $\rho_L(Y, a)$ for (*a*) $a = -\pi/4$, (*b*) $a = 0$, (*c*) $a = +\pi/4$, (*d*) $a = +\pi/2$. Full curves: theory [1] of section 2; bold dots: billiard eigenstates. The inset in (*c*) is a magnification of the peak near $Y = \pi/4$, arising from the ghost lines.

them to 320 points on the quarter circle and its connected straight segment with unit length; this corresponds to about nine boundary points per wavelength. A criterion for accuracy was the mean-square deviation from the boundary conditions at 3000 other boundary points. In this way, we captured about 74% of the states (about 35 states) in the chosen k interval for each value of a except $a = 0$, for which we captured about 36% of the states (17 states). Our ensemble included some 'bouncing-ball' states, to which the theory does not apply (because the directions of plane waves in the modal superposition are concentrated near the normal to the straight sides); nevertheless, we included them, because they were too few (about 10%) to significantly affect the comparison with theory.

Figure 1 shows a typical such state, for $a = +\pi/4$. This case is chosen to show the ghost nodal lines (figure 1(*b*)) and to illustrate how this feature is hard to discern in the intensity plot of figure 1(*a*).

For an individual eigenstate and a given value of a, the nodal line density involves a sum over intersections of nodal lines with the shrunken image of ∂D consisting of the locus of points at distance Y/k from the closest point on ∂D. To get $\rho_L(Y, a)$, each intersection in the sum must be weighted by $1/\cos\gamma$, where γ is the angle between the normal $\mathbf{n}$ and the nodal line. As mentioned at the end of section 2, this procedure makes sense only if Y/k is less than the minimum radius of curvature of ∂D; in the present case, this implies $Y < 42.5$. Finally, the resulting densities were averaged over all eigenfunctions in the sample. For M states, the number S of independent samples for each Y near the boundary can be estimated as M times the number of half-wavelengths around the boundary, this gives $S \sim 5000$, except for $a = 0$ where the smaller number of eigenstates gives $S \sim 2500$. Therefore, we can expect fluctuations $1/\sqrt{S}$ of a few per cent.

Figure 2 shows how accurately the billiard eigenstates fit the Gaussian random theory for the nodal line density $\rho_L(Y, a)$, even deep inside D and for the ghost nodal lines (inset

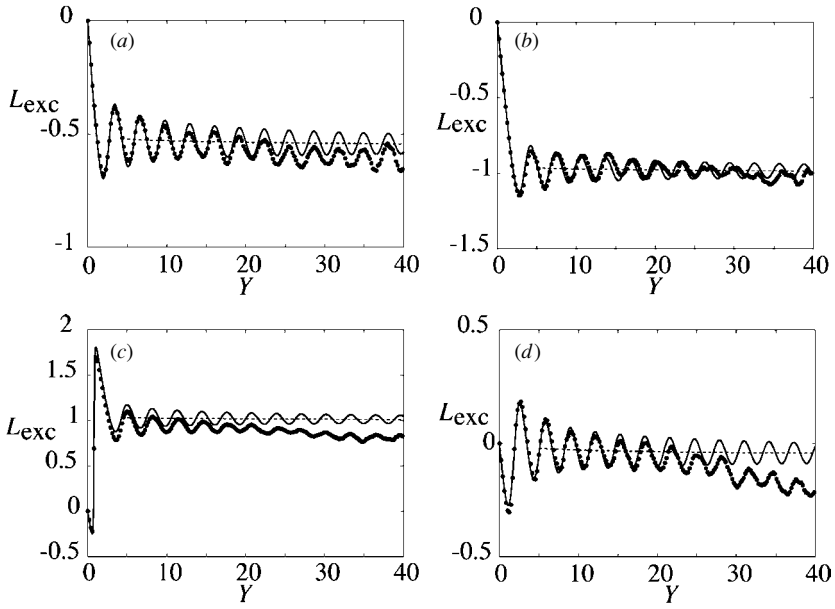

Figure 3. As figure 2, for the excess nodal line density $L_{\rm exc}(Y, a)$. The dashed curves show the non-oscillatory part of the asymptotic formula (8), with constants $C_{\rm L}(-\pi/4) = -0.507$, $C_{\rm L}(0) = -0.948$, $C_{\rm L}(+\pi/4) = 1.049$, $C_{\rm L}(+\pi/2) = -0.006$.

in figure 2(c)). The more discriminating test of the excess density $L_{\rm exc}(Y, a)$ is shown in figure 3. Except for figure 3(c), corresponding to $a = +\pi/4$, the fits are excellent for Y less than about 20, but degrade for larger Y, corresponding to points deep inside D, where the theory can hardly be expected to apply, with $L_{\rm exc}$ becoming smaller than the theoretical predictions. We conjecture that the poorer fit for $a = +\pi/4$ results from a failure to capture all the density in the ghost peak.

4. Discussion

The theory that we have been comparing with numerical experiments is analogous to the boundary correction [12] to the Weyl rule for the eigenvalue counting function. The rather good agreement gives further strong support to the Gaussian random-wave hypothesis for the eigenfunctions of classically chaotic quantum systems.

Our tests have been based on averaging over an ensemble of states. However, the Gaussian random hypothesis is more discriminating, in the sense that it should also apply to asymptotically high individual chaotic states. This test is still lacking; to get comparable accuracy to that reported here would require numerically computing the nodal statistics of single states near the 30 000th.

Just as the boundary correction to the Weyl rule is the first term of an infinite (divergent) series [13], so we expect the boundary corrections considered here to be the first in a series of corrections to the nodal line density statistics, with successive contributions capturing more subtle features of ∂D. A start has been made [14] on the next correction, which incorporates the curvature of ∂D, at least for Dirichlet and Neumann boundary conditions. It would be interesting to establish the structure of the full series of corrections, involving higher powers of curvature and rates of change of curvature.

Acknowledgments

MVB is supported by the Royal Society. HI acknowledges support by a Grant-in-Aid for the 21st Century COE 'Frontiers of Computational Science' (Japan).

References

[1] Berry M V and Ishio H 2002 Nodal densities of Gaussian random waves satisfying mixed boundary conditions *J. Phys. A: Math. Gen.* **35** 5961–72
[2] Berry M V 1977 Regular and irregular semiclassical wave functions *J. Phys. A: Math. Gen.* **10** 2083–91
[3] Voros A 1979 *Stochastic Behaviour in Classical and Quantum Hamiltonian Systems* vol 93 ed G Casati and J Ford (Berlin: Springer) pp 326–33
[4] Berry M V 1983 *Semiclassical Mechanics of Regular and Irregular Motion in Les Houches Lecture Series* vol 36 ed G Iooss, R H G Helleman and R Stora (Amsterdam: North-Holland) pp 171–271
[5] O'Connor P, Gehlen J and Heller E J 1987 Properties of random superpositions of plane waves *Phys. Rev. Lett.* **58** 1296–9
[6] Heller E J 1991 *Wavepacket Dynamics and Quantum Chaology in Chaos and Quantum Physics, Les Houches Lecture Series* vol 52 ed M-J Giannoni, A Voros and J Zinn-Justin (Amsterdam: North-Holland) pp 547–663
[7] Saichev A I, Ishio H, Sadreev A F and Berggren K-F 2002 Statistics of interior current distributions in two-dimensional open chaotic billiards *J. Phys. A: Math. Gen.* **35** L87–93
[8] Blum G, Gnutzmann S and Smilansky U 2002 Nodal domains statistics—a criterion for quantum chaos *Phys. Rev. Lett.* **88** 114101
[9] Berry M V 2002 Statistics of nodal lines and points in chaotic quantum billiards: perimeter corrections, fluctuations, curvature *J. Phys. A: Math. Gen.* **35** 3025–38
[10] Berry M V and Dennis M R 2000 Phase singularities in isotropic random waves *Proc. R. Soc. A* **456** 2059–79
[11] Wolfram S 1996 *The Mathematica Book* (Cambridge: Cambridge University Press)
[12] Baltes H-P and Hilf E R 1976 *Spectra of Finite Systems* (Mannheim: B-I Wissenschaftsverlag)
[13] Berry M V and Howls C J 1994 High orders of the Weyl expansion for quantum billiards: resurgence of periodic orbits, and the Stokes phenomenon *Proc. R. Soc. A* **447** 527–55
[14] Wheeler C T 2005 Curved boundary corrections to nodal line statistics in chaotic billiards *J. Phys. A: Math. Gen.* **38** 1491–504